Tetrahedron 66 (2010) 2322–2330

Contents lists available at ScienceDirect

Tetrahedron

journal homepage: www.elsevier.com/locate/tet

DFT, ab initio, NMR, and NBO analyses of N^{α}-substituted hydrazino acetamides: Experimental vs theoretical values

Hossein A. Dabbagh [a,*], Elham Rasti [a], Philippe Le Grel [b], Alexandre Hocquet [c]

[a] Department of Chemistry, Isfahan University of Technology, 8415483111 Isfahan, Iran
[b] UMR CNRS-Université Rennes I 6226, 35042 Rennes, France
[c] UMR CNRS-INPL 7568, B.P. 451, 54001 Nancy, France

ARTICLE INFO

Article history:
Received 17 October 2009
Received in revised form 3 January 2010
Accepted 1 February 2010
Available online 4 February 2010

Keywords:
Hydrogen bond
Hydrazinoturn
NBO analysis
Aza-β^3-peptide
NMR

ABSTRACT

We studied the DFT (B3LYP) and HF at 6-31+G/6-31+G** levels of theory in order to throw light on the conformation, structure, intramolecular hydrogen bond network, as well as proton and nitrogen NMR (GIAO method) of a series of model primary amides in the gas phase and/or in solution (chloroform, methanol, water, dimethyl sulfoxide, and heptane). In this manner, it was possible to show that the amidic group of these model compounds acts as the H-bond donor and interacts with two different H-bond acceptors, thus stabilizing the C_8 pseudocycle. The study was conducted to gain a better understanding of the conformation (both experimentally and theoretically) adopted by hydrazino acetamides (model compounds for aza-β^3-peptides). In the light of this, we were able to explain why aza-β^3-peptides develop a different H-bond network in comparison to their isosteric β^3-peptide analogues (an extension of the β-peptide concept).

1. Introduction

We know of hydrogen bonds that are so strong that they resemble covalent bonds (quasi-covalent hydrogen bonds) in most of their properties, and some of others are so weak that they can hardly be distinguished from van der Waals interactions.[1] In many chemical and biochemical processes, hydrogen bonding is one of the most important interactions that occurs in aqueous and polar environments. The 'O···HO, O···HN' are two very important types of hydrogen bonds; however, the heteronuclear NH···O system is even more important than the homo nuclear OH···O bond because of its important role in living systems.[2a–d]

Ab initio calculations imply that amide–amide hydrogen bonding is strongest when the NH···O angle approaches linearity (optimum values are calculated to be around 160°). Hydrogen bond energy, however, appears to be less sensitive to the C=O···H angle as long as this angle is greater than 90°.[3,4] One of the challenging issues in molecular design is the control of three-dimensional structures.[5] Hydrazinopeptides[6] and aza-β^3-peptides[7] (Scheme 1) are viewed as promising pseudopeptides in order to build self-organizing foldamers,[8] mimicking the secondary structure of biomolecules.

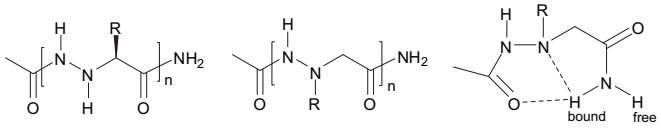

Scheme 1. Hydrazino peptides (left), aza-β^3-peptides (middle), and Hydrazinoturn, with the 'bound' hydrogen atom and the reference 'free' hydrogen atom (right) illustrated.

The introduction of supplementary nitrogen inside the peptide backbone allows new intramolecular interactions involving either this nitrogen atom or the one directly bound to it. These interactions (a putative bifurcated hydrogen bond) reinforce the formation of an eight-membered cyclic hydrogen-bond. These networks of hydrogen bonding, called 'hydrazinoturn', occur in this family of molecules[9] and have been viewed as a major force leading to the secondary structures of certain families of foldamers (Scheme 1).

Recently, Salaün et al. investigated the role of hydrogen bonding in aza-β^3-peptide structure using NMR structural study of model hydrazine acetamide compounds mimicking the aza-β^3-peptide backbone to characterize the 'hydrazinoturn' with a measurable change in chemical shift for the hydrogen atom involved.[10] Simo et al. examined the role of the hydrogen bonding network in hydrazino peptides and aza-β^3-peptides by an AIM topological analysis of the electron density.[11] Recently, we reported the quantum chemical analysis of the effect of triazene acetamide substitution.[12a]

* Corresponding author. Tel.: +98 311 391 3257; fax: +98 311 391 2350.
E-mail address: dabbagh@cc.iut.ac.ir (H.A. Dabbagh).

0040-4020/$ – see front matter © 2010 Elsevier Ltd. All rights reserved.
doi:10.1016/j.tet.2010.02.007

Bax et al. reported the determination of amide N–H equilibrium bond length using concerted dipolar coupling measurements.[12b] Timmoms and Wipf reinvestigated the structure of a cyclic amide diazaphenanthrene alkaloid (samoquasine A) using DFT calculation of ^{13}C NMR shifts.[12c] Dabbagh et al. investigated the experimental and quantum chemical diastereoselective formation of eighteen-membered hydrogen bonded pseudocycles.[13a] They reported the experimental and theoretical results for an eleven-membered bifurcated hydrogen-bonded pseudocycle for methyl-2,4-dimethoxy-salicilate (a potential *anti*-tumor agent).[13b] Kleinpeter and Frank studied the steric substituent effect on the intensity of the push-pull effect in substituted alkynes using DFT calculation of ^{13}C NMR shifts.[13c] Jimenez-Fabiant et al. investigated the molecular structure and the intramolecular hydrogen bonding of β-aminoacroleins at MP2 and B3LYP levels of theory. They utilized AIM and NBO analyses to characterize the nature of hydrogen bonding in these systems. They also demonstrated that the topological parameters could be applied to estimate the hydrogen bond strength.[13d]

The aim of the present study is to apply quantum chemical methods to 14 sample molecules described by Salaün et al.[10] and to compare the results of experimental NMR chemical shift differences $\Delta\delta$ with those of a theoretical proton NMR. The optimized geometry and the energy minima and maxima of the compounds **1**–**9c** (Scheme 2) were computed both in the gas phase and in solution (chloroform, methanol, water, dimethyl sulfoxide, and heptane). Furthermore, the X-ray structural features of two of these molecules[10] were compared with computed values.

2. Computational methods

All of the structures of primary amides studied in this work were optimized by Hartree-Fock (HF) and density functional method (DFT) at B3LYP level applying 6-31+G and 6-31+G** basis sets individually. The density functional method adopted here is B3LYP, i.e., Becke's three-parameter hybrid functional using Lee–Yang–Parr[14,15] correlation function. The various levels at which optimizations were performed included HF/6-31+G, HF/6-31+G**, B3LYP/6-31+G, and B3LYP/6-31+G** methods. All calculations reported were carried out using GAUSSIAN 03 software.[16] The starting geometry for each optimization was performed independently and/or chosen from the X-ray diffraction study results in Ref. 10. Potential energy scan (PES) studies of these compounds were performed in order to obtain the internal barrier to rotation at HF/6-31G level. The geometry obtained from the minimum energy of these compounds was computed at the DFT level of theory (B3LYP/6-31+G**), which included the diffuse shells as well as d and p polarization functions. The chemical shift differences was computed at the same level of theory using the gauge-invariant atomic orbital (GIAO)[17] method and referenced to TMS shielding values also calculated at HF/.6-31G*. The population of the orbitals and the occupation of relevant orbitals of these molecules were calculated by NBO analysis[18a,b] and by reference to B3LYP/6-31+G** molecular geometries.

3. Results and discussion

The 14 molecules selected for this study are listed in Scheme 2. These molecules were selected because **1** and **9c** showed an eight-membered bifurcated hydrogen bonded pseudocycle network. The influence of replacing one nitrogen atom by a carbon atom was investigated in molecules **9a**, **9b**, and **9c**. Molecules **3**, **4**, and **5** showed an O···H hydrogen bond but no N···H hydrogen bond. Molecules **6a** and **6b** showed no internal hydrogen bond. Molecule **6b** rather than **6a** here serves as the reference because

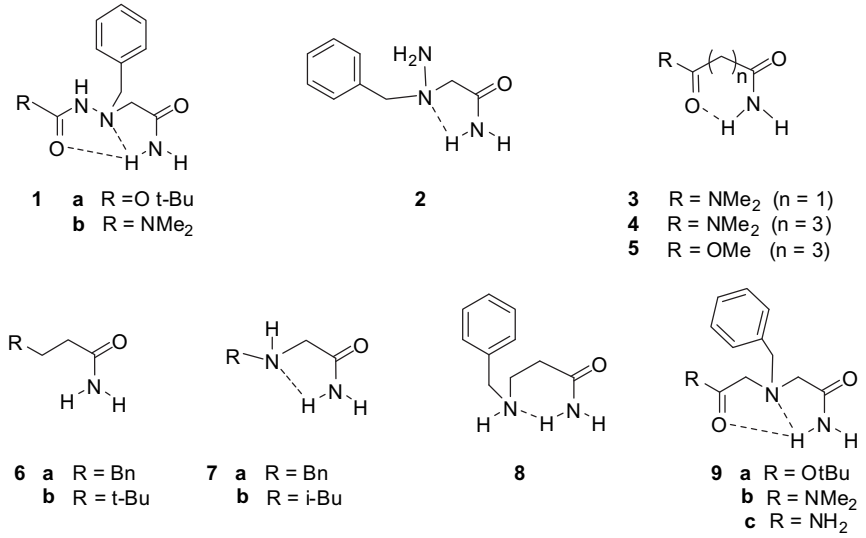

Scheme 2. The 14 molecules for which structures have been investigated in this study.

Finally, in order to throw light on the intramolecular hydrogen bond network of these molecules, conformational analysis was performed for each sample by rotation around the bond next to the amide group. The objective of the study was to a gain a better understanding of the H-bond interaction in a more general context.

it has no internal hydrogen bond and does not experience any anisotropic effect by the phenyl group. Molecule **2** showed an N···H hydrogen bond but no O···H hydrogen bond. Molecules **7** and **8** showed two folded states with O···H and N···H hydrogen bonds, respectively. However, the dominant conformers of **7** and **8** showed NH···N hydrogen bonds. Molecules **1a**, **1b**, **2**, **3**, **4**, **5**, **6a**, **7a**, **7b**, **8**, **9a**, **9b**, and **9c** are those of **1a**, **1b**, **1c**, **2a**, **3a**, **4a**, **5**, **6a**, **6b**, **7**, **8a**, **8b**, and **8c** in Ref. 10, respectively. We investigated the structural parameters of the molecules, which were influenced by the internal hydrogen bonding network (C═O···HN and HN···HN). In this respect, we defined, as also reported in Refs. 10 and 11, two geminal amidic protons for the comparison of structural parameters: the bonded NH (H_b) relative to the 'free' one (H_f) (Scheme 3).

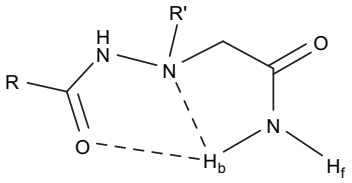

Scheme 3. Hydrazinoturn hydrogen bonding network, showing the 'bound' hydrogen atom and the reference 'free' hydrogen atom.

The total energy, dipole moment, ratio of energy, and ratio of dipole moment of optimized substituted hydrazino or primary acetamides of structures reported in Table S1 were optimized at HF/6-31+G, HF/6-31+G**, B3LYP/6-31+G, and B3LYP/6-31+G** levels. The intramolacular hydrogen bond length and bond angle (C═O···H–N and HN···HN) of **1**–**9c** were calculated at HF/B3LYP/6-31+G/6-31+G** levels, which complement those of Ref. 11 at B3LYP/6-31++G** level (where available) (Table S2).

There are two intramolecular H-bonds in molecules **1a**, **1b**, **9a**, **9b**, and **9c**: (NH···N) and (NH···O). The resulting H-bond gives rise to a five- and eight-membered hydrogen-bonded pseudocycles. The (NH···O) and (NH···N) bond lengths for compound **1a** are 2.09 Å and 2.39 Å, those for compound **1b** are 2.00 Å and 2.45 Å, those for compound **9a** are 2.19 Å and 2.50 Å, those for compound **9b** are 2.00 Å and 2.50 Å, and those for compound **9c** are 2.12 Å and 2.52 Å, respectively using the B3LYP/6-31+G** method. Molecules **1a**, **1b**, **9a**, **9b**, and **9c** are very similar: The O···H and N···H distances, as well as the NH···O and NH···N angles, indicate a bifurcated hydrogen bond, as has also been summarised in Ref. 10. Comparison of **1a** and **1b**, on the one hand, and **9a**, **9b**, and **9c**, on the other, show small differences between the O···H intramolecular hydrogen bonding networks and larger differences for the N···H hydrogen bond. Molecules **1a** and **1b** experienced stronger internal hydrogen bonding, which could be due to the presence of a β nitrogen atom in molecule **1a** and **1b**. This nitrogen atom is not present in molecules **9a**, **9b**, and **9c**. This could be related to the lone-pair electron repulsion in the N–N fragment. This structural constraint is known to favor an orthogonal arrangement between the lone pairs. In this sense it restrains, to some extent, the flexibility of the hydrazino fragment, acting as a type of braking mechanism against the rotation about the N–N bond. When rotation occurs, lone pairs tend to eclipse and electronic repulsion increases. Part of the repulsion could be released if the N^{β} lone-pair conjugated efficiently with the adjacent carbonyl group. The latter would become more polarized, thus making it a stronger H-bond acceptor.[19] In other words, a carbamate moiety double bonded oxygen atom would be a better H-bond acceptor than an ester or an amide one. Molecules **1a** and **1b** revealed a greater propensity to stabilize the bifidic arrangement (two hydrogen-bonded pseudocycles) than **9a**, **9b**, and **9c**. Secondly, for molecules **4** and **5**, which prefer the eight-membered hydrogen-bonded pseudocycle, and both of which possess an intramolecular O···H hydrogen bond but no N···H hydrogen bond, the reading of Table S2 indicates a strong intramolecular hydrogen bonding, particularly for molecule **4**. We can deduce from the figures that the amide function oxygen atom (in molecule **4**) is a more efficient hydrogen bond acceptor than the ester function oxygen (in molecule **5**), in agreement with the results in Ref. 10. Molecules **7a** and **7b** exhibit similar intramolecular hydrogen bonds. A clear intramolecular hydrogen bond exists between H and N, thus forming a C_5 pseudo ring. Intramolecular hydrogen bonding in molecule **8** reveals a C_6-membered pseudo ring, the intramolecular hydrogen bonding network obviously prefers the C_6 pseudo ring to the C_5 pseudo ring in terms of the efficiency of hydrogen bonding (Scheme 2).[10,11]

In the next phase, the differences of computed chemical shift differences ($\Delta\delta$) of the amidic protons were compared with experimental values (conformation of N^{α}-substituted hydrazine acetamides in $CDCl_3$, the analysis of $\Delta\delta$ between amidic hydrogens, and correlation to the conformation of aza-β^3-peptides[10]). Unfortunately, there was no experimental value reported for the other solvents used in our calculations. In these cases, we simply discussed the effect of increasing polarity of the solvent on chemical shift differences.

The initial strategy was to compute the NMR values from the optimized geometry (at DFT/B3LYP/6-31+G**) of each molecule using X-ray input parameters (Table S2). Much to our surprise, the calculated $\Delta\delta$ values showed large deviations from those of the experimental values. In the next step, the effect of basis set on computed chemical shift differences ($\Delta\delta$) of amidic protons was studied. The geometry of molecules optimized at B3LYP/6-31+G** level was selected to compute $\Delta\delta$ using various basis sets (HF/6-31G, DFT/B3LYP/6-31G, and DFT/B3LYP/6-31+G**) (Table 1). These clearly indicate that the computed NMR values of these systems depend on the geometry[20] of the molecules rather than on the applied basis set. We, therefore, calculated $\Delta\delta$ in solution (chloroform, methanol, water, dimethyl sulfoxide, and heptane) at HF/6-31G/GIAO level of theory (Table S3). These observations promoted a search for conformer (s) to produce NMR values similar to those of experimental findings. To achieve this goal, the potential energy scan (PES) was performed for these compounds by rotating about the bond next to the primary amidic moiety (–C–C–CO–NH_2 group for compounds **3**, **4**, **5**, and **8**) and (–N–C–CO–NH_2 group for compounds **1a**, **1b**, **2**, **7a**, **7b**, **9a**, **9b**, and **9c**).

Table 1
Experimental and calculated proton NMR chemical shift differences at HF/DFT/6-31G and DFT/6-31+G** in gas phase of **1**–**9c**[a]

Amide Proton NMR Chemical Shift Difference ($\Delta\delta$)				
Com.	Expt.[b]	Calculated in gas phase[c]		
	$CHCl_3$	HF/6-31G	DFT/6-31G	DFT/6-31+G**
1a	2.60	4.17	4.22	4.25
1b	3.10	4.68	4.64	4.74
2	1.60	1.88	2.25	1.92
3	2.30	2.21	2.45	2.43
4	0.70	3.18	3.23	3.24
5	0.15	2.60	2.74	2.49
7a	1.60	2.28	2.62	2.29
7b	1.75	2.51	2.92	2.59
8	2.15	3.74	3.85	3.715
9a	2.10	3.48	3.61	3.47
9b	2.60	4.15	4.18	4.012
9c	1.2	3.85	3.91	3.75

[a] Molecules **1**–**9c** were optimized at B3LYP/6-31+G**.
[b] Ref. 10.
[c] Reference to TMS at HF/6-31G (d)/GIAO.

The conformer (s) with minimum energy was extracted from the PES plot and optimized at DFT/B3LYP/6-3+G**. The structural parameters (H-bond length and H-bond angle) of the minima conformers (optimized at DFT/6-31+G**) are listed in Table S4.

The ^{1}H NMR chemical shift differences of this conformer was computed at the same level of theory both in the gas phase and in solution. These results were compared with experimental values (Tables 2 and S5).

One example of conformational analysis (for **7a**) is discussed below for illustration. The rotation about the C(2)–C(3) bond of molecule **7a** gave two maxima and two minima energy conformers. The energy maximum conformer at 290° experienced the repulsion of –NH_2 and –Ph groups but no intramolecular H-bonding. The conformer at 80° was slightly more stable (0.60 kcal/mol) than the conformer at 290°. The conformer at 350° had the lowest energy (a result of intramolecular H-bonding). The resulting H-bond gave rise to a five-membered hydrogen-bonded pseudocycle. The

Table 2
Computed amidic proton NMR chemical shift differences ($\Delta\delta$) and their natural charges of optimized minima conformer of **1–9c**

Com.	Dihedral (φ)[a]	$\Delta\delta$ (ppm)		Natural Charges (q)		Δq
		Gas[b]	$CHCl_3$ (Exp.)[c]	H_b	H_f	H_b H_f
1a	61.8	3.22 (3.36)	2.85 (2.6)	0.449	0.426	0.024
1b	23.7	3.87 (3.89)	3.52 (3.10)	0.452	0.426	0.026
2	329.3	1.93 (2.01)	1.83 (1.6)	0.439	0.435	0.004
3	30.1	2.63 (2.70)	2.23 (2.3)	0.456	0.427	0.029
4	119.0	0.54 (0.52)	0.74 (0.7)	0.426	0.428	-0.002
5	315.2	0.03 (0.09)	0.29 (0.15)	0.417	0.432	-0.015
7a	350.2	1.85 (1.94)	1.77 (1.6)	0.433	0.429	0.004
7b	346.3	1.99 (2.19)	1.93 (1.75)	0.435	0.429	0.006
8	302.9	2.26 (2.33)	2.19 (2.15)	0.436	0.425	0.011
9a	50.9	2.40 (2.32)	2.11 (2.10)	0.444	0.427	0.017
9b	5.9	3.11 (3.09)	2.83 (2.6)	0.455	0.433	0.021
9c	68.6	1.71 (1.65)	1.52 (1.20)	0.441	0.427	0.014

[a] X–C–C—CO–NH_2 (X=C and N).
[b] Values in parenthesis are the calculated proton NMR at DFT/6-31+G**/(GIAO).
[c] The experimental $\Delta\delta$ values are in parenthesis.

conformer at 180° also experienced an internal H-bond between the hydrogen of the amine and the oxygen of the amidic group (NH···O=C). The H-bond acceptors in conformers at 180° and 350° were the oxygen of the amidic group (C=O) and the nitrogen of the amine (NH), respectively (Figs. 1 and 2).

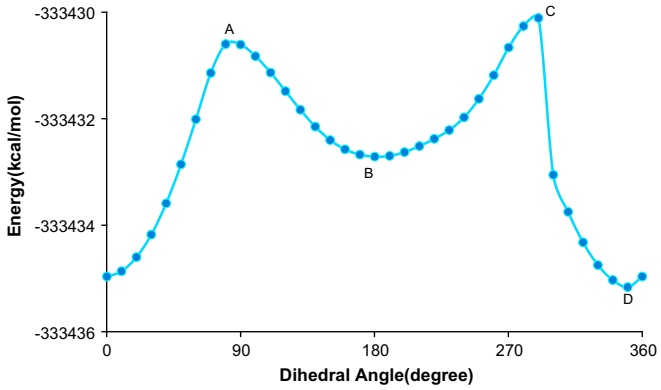

Figure 1. Plot of dihedral angle vs (calculated) energy of compound **7a**.

An excellent correlation was observed between experimental and calculated chemical shift differences values $[(\Delta\delta)_{calcd}=0.9685(\Delta\delta)_{exp}-0.0397$ ($R^2=0.9757$)] (Fig. 3). This correlation indicates that the correct geometry had been selected for NMR calculations. The computation of ^1H chemical shifts is usually rather poor; the methodology used herein is aimed for chemical shift differences hence most of the systematic errors in chemical shift calculations are canceled out in subtraction. Poor correlation was observed when experimental absolute chemical shifts were plotted vs the computed absolute chemical shifts (Figs. S1 and S2). The absolute ^1H chemical shift of the two amidic hydrogens (H_b and H_f) of the minima conformers of **1–9c** (which was optimized at DFT/6-31+G** in gas phase at HF/6-31G level of theory) are listed in Table S6.

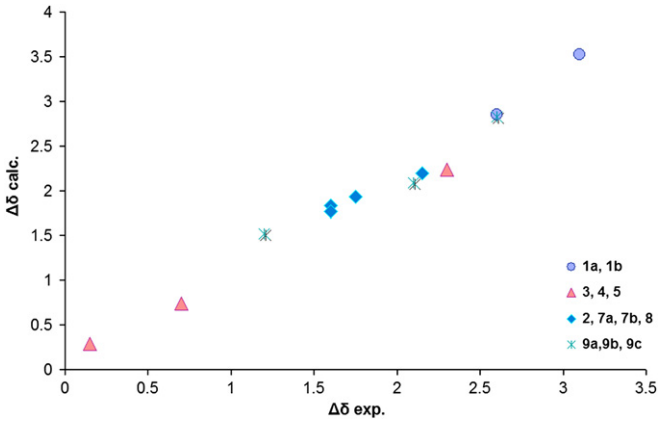

Figure 3. Correlation of experimental[10] and computed ^1H chemical shift differences ($\Delta\delta$) of the amidic protons H_b and H_f.

The hydrazino acetamide **1a** reveals a much higher $\Delta\delta$ value (2.85 ppm) than the experimental one ($\Delta\delta$=2.60 ppm). Since this compound folds into an eight-membered hydrogen-bonded pseudocycle, the value of **1a** implies that specific structural features must be present, displacing the propensity toward the folded state. Both five-membered and eight-membered pseudocycles could contribute to the folding process in a competitive way. The aza-analogues **1a** ($\Delta\delta$=2.85 ppm) and **1b** ($\Delta\delta$=3.52 ppm) showed higher calculated $\Delta\delta$ values in comparison to compounds **9a** and **9b**. This argues against a significant population of a C_6 conformation.

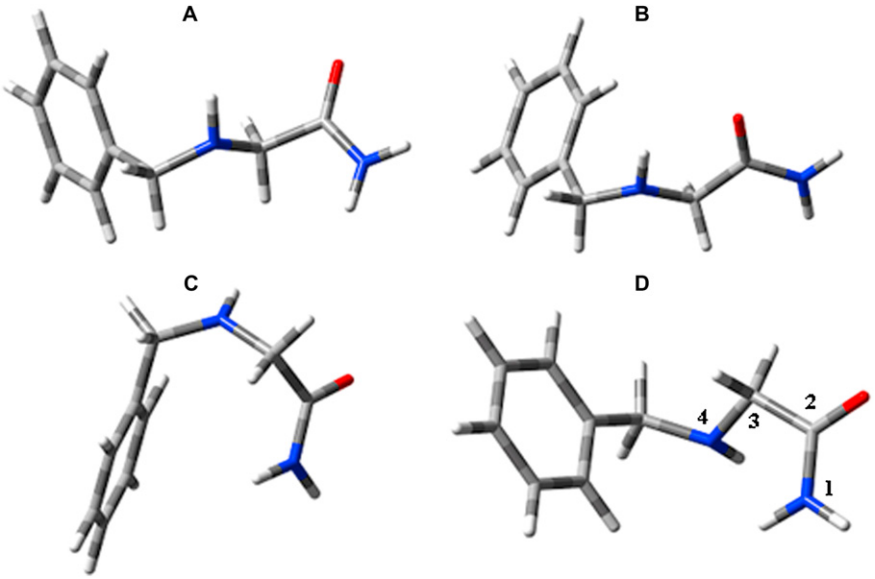

Figure 2. (**A**) The next highest energy maxima conformer (~80°), (**B**) the next lower energy minima conformer (~180°), (**C**) the highest energy maxima conformer (~290°), and (**D**) the lowest energy minima conformer (~350°) of **7a**.

The increase of 0.67 ppm observed for N^{α}-substituted hydrazino acetamides **1a** and **1b** reveals a greater propensity to stabilize the bifidic arrangement. We assume that this must be related to the lone-pair electron repulsion in the N–N fragment (Ref. 10).

The $\Delta\delta$ value (1.83 ppm) of **2** was obtained at a dihedral angle of 185° where a five-membered conformation contributes to the folding process in a competitive way. As the $\Delta\delta$ value of **2** is closer to that of **7a** (1.77 ppm) than to that of **8** (2.19 ppm), it seemingly indicates a preference for a five-membered hydrogen-bonded pseudocycle or may be the result of the lone-pair electron repulsion with an exocyclic terminal nitrogen.

The $\Delta\delta$ values of compounds **3**, **4**, and **5** were calculated to be 2.23, 0.74, and 0.29 ppm. These values are in excellent qualitative agreement with the experimental values of 2.30, 0.70, and 0.15 ppm, respectively, reported by Salaün et al. Proton NMR of **3** was computed for the conformer at the dihedral angle of 30.10°. Compound **3** predominantly exists as a six-membered hydrogen-bonded pseudocycle. The NMR $\Delta\delta$ value of **4** was calculated (0.74 ppm) for the conformer at 119.03° in chloroform. In the solvent, the predominant conformer (at dihedral angel 119°) with a weak intramolecular H-bond does not experience the *gauche* repulsion. The calculated NMR for the conformer at the dihedral angle of 69° exhibiting hydrogen bonding deviated from the experimental NMR. This was the result of *gauche* repulsion. In other words, the steric hindrance overcomes the stability exerted by H-bond. A similar observation was made for **5** but with smaller $\Delta\delta$. This conformation (at a dihedral angle of 315.2°) allows H-bonding between NH_2 and the ester group (the ester group is less polarized and a weaker hydrogen bond acceptor than the amide group). The much larger value observed for **3** compared to **4** is due to the shift of the equilibrium toward the six-membered pseudocyclic folded state (Table 2).

In the case of **3**, by increasing polarity from the gas phase to water, intermolecular H-bonding was favored (H_f shifted downfield, 3.77 ppm) while H_b was almost unaffected (trapped in an intramolecular H-bond, 5.86 ppm) (Fig. 4). The same tendency was reported experimentally at higher concentrations or when the amounts of DMSO (d_6) were increased.[10] For **4** and **5**, both NHs moved downfield at higher polarity levels of the solvent, confirming that the unfolded state is predominantly populated, Ref. 10 (Fig. 4). In the unfolded state, H_b formed a stronger H-bond (deshielded) with the polar solvents because of the less repulsion between the incoming solvent and the carbonyl.

To verify if the steric hindrance alone could differentiate the two amidic protons, Salaün et al. prepared the sterically comparable 4-phenylbutyramid **6a** in which no significant H-bond acceptor was present. The experimental zero $\Delta\delta$ of **6a** revealed no interaction. In this work, a very small $\Delta\delta$ (0.22 ppm) value in chloroform was calculated for **6a** indicating a small interaction (H-bonding with aromatic π-system)[21] between the phenyl and the amidic protons. In contrast to compound **6a**, the $\Delta\delta$ value of the isosteric amide **7a** is 1.77 ppm, and the $\Delta\delta$ of the upper homolog **8** is 2.19 ppm. A strong anisotropic effect for **7a** by the phenyl ring on the $\Delta\delta$ value was observed or **8** can be eliminated, as $\Delta\delta$ is 1.93 ppm for **7b**. These values are in excellent qualitative agreement with experimental values.[10] Nevertheless, it is clear that the primary amides of **7a** and **7b** substantially interact with the lone-pair of the sp^3 nitrogen. The resulting H-bond gives rise to a five-membered hydrogen-bonded pseudocycle. To further test the steric factor and eliminate any possible H-bonding interaction between the phenyl and the amidic protons of **6a**, the $\Delta\delta$ of proton NMR of 4,4-dimethylpentanamide **6b** was examined to obtain a value of 0.26 ppm in chloroform.

For the tertiary amine **9a**, the $\Delta\delta$ value (2.11 ppm) calculated at the dihedral angle of 50.9° is in excellent qualitative agreement with the experimental value (2.10 ppm). The tertiary amine **9b** combines the structural features present in compounds **4** and **7a** (Scheme 2). The $\Delta\delta$ value of **9b** (2.83 ppm) is higher than the sum of

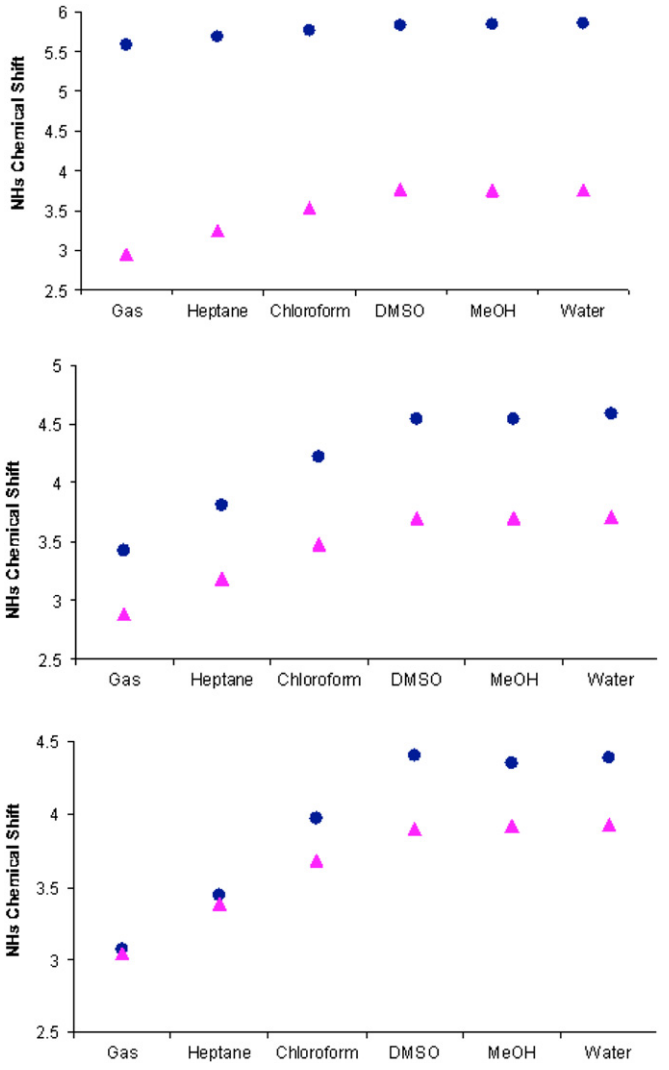

Figure 4. NH_b (●) and NH_f (▲) computed chemical shifts of **3** (top), **4** (middle) and **5** (bottom) as a function of solvent polarity.

the individual values (0.74+1.77). Assuming that compound **9b** can adopt a bifidic folded state, the nonlinearity observed can be interpreted as the result of a more favorable entropic situation. In such a conformation, the two H-bond acceptors, although competitive, mutually reinforce their efficiencies by restraining the flexibility of the molecule.[10] Considering the respective $\Delta\delta$ values of **4** and **7a**, it is reasonable to propose that the five-membered hydrogen-bonded pseudocycle is the most important contributor to the folding process, since its most favorable formation makes the subsequent participation of the carbonyl group easier. This is confirmed by the $\Delta\delta$ value of compound **9a**, which reaches 2.11 ppm (theory for conformer at 50.9°), despite the presence of the significantly less polarized ester group. For the symmetrical tertiary amine **9c**, the $\Delta\delta$ value (1.52 ppm) calculated from the conformer at a dihedral angle of 68.6° is in qualitative agreement with the experimental value (1.20 ppm) and is almost half the value reported[10] for tertiary amide **9b** (2.83 ppm). This makes sense since each amide group acts alternatively as a H-bond donor and a H-bond acceptor. The deviation between the experimental (1.20 ppm) and the expected (1.52 ppm) values was a result of the difference in polarity between primary and tertiary amides.

Furthermore, there is a linear relationship between the increase in $\Delta\delta_{Hb,Hf}$, $\Delta q_{Hb,Hf}$, and the strength of hydrogen bond (Fig. 5). The higher the differences in chemical shift and charge polarization of

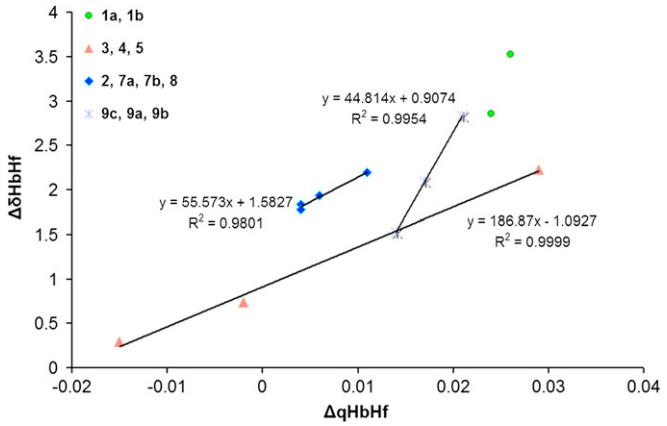

Figure 5. Correlation between the ^{1}H chemical shift differences ($\Delta\delta_{Hb,Hf}$) and the charge density differences ($\Delta q_{Hb,Hf}$) of amidic hydrogens.

amidic protons, the stronger the hydrogen bond. This increase is more pronounced for molecules **1** and **9** both of which are involved in a C_8 pseudocycle H-bond network system.

The results of NBO analysis (occupation number for the assignments and their corresponding orbital energies) for these systems are given in Table S7. In this Table, the NBO occupation numbers are reported for σ (N–H_b) bonds; σ* (N–H_b) antibonds; the oxygen lone pairs, n O; the nitrogen lone pairs, n N; and their respective orbital energies, *E*. In the NBO analysis of hydrogen bonded systems, the charge transfer between the lone pairs of proton acceptor and antibonds of proton donor is highly important. The results of the NBO analysis (Table S7) shows that in the chelated structures of these molecules, two lone pairs of oxygen atom (n_2 O) and (n_1 N) participate as donors and σ* (N–H_b) antibonds serve as acceptors.[13c,13d]

There is also a linear correlation between the quotient ($\sigma^*_{N-Hb}/\sigma_{N-Hb}$) and the NH···O and NH···N bond distance (Fig. 6). This plot predicts that the quotient (σ*/σ) of the N–H_b bond (N–H_b of primary amidic was involved in intramolecular hydrogen bonding) and the charge polarization at two hydrogen (H_b H_f) correlate well as descriptors of the hydrogen bond strength.

The molecular orbital *anti*-bonding σ*of N–H_b of hydrazinoturns **1a**, **1b**, **9a**, and **9b** are depicted in Figure 7. These orbitals noticeably verified the greater intramolecular hydrogen bonding in molecules **1b** and **9b** than in **1a** and **9a**, and the greater electron density between the atoms involved in hydrogen bonding.

Finally, the nitrogen chemical shift of primary amidic nitrogen (which was involved in intramolecular hydrogen bonding) of compounds **1**–**9c** was calculated at HF/6-31G/GIAO level of theory (reference to NH_3 at HF/6-31G (d) GIAO) (Table S8).

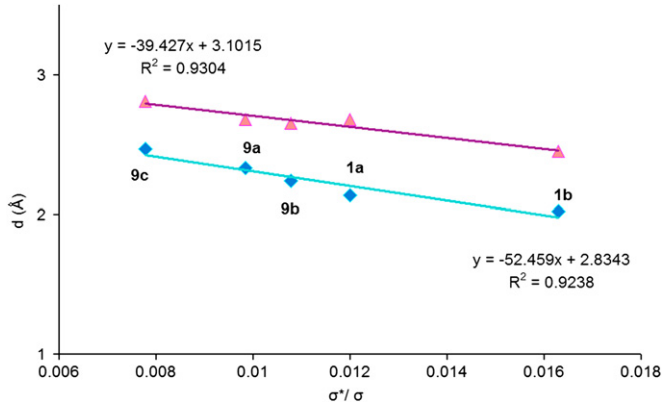

Figure 6. Dependence of the NH···O (◆) and NH···N (▲) bond distance (in a C_8 pseudocycle) on the occupation quotients of the *anti*-bonding σ* and bonding σ orbitals of N–H_b bond.

Unfortunately, there was no experimental nitrogen NMR value available for comparison. However, comparison of the nitrogen chemical shifts of **1a**, **5**, and **9a** both in the gas phase and in solution (chloroform, methanol, water, dimethyl sulfoxide, and heptane) shed some light on the effect of pseudocycles and β-nitrogen on the extent of H-bonding (Table S8). All three molecules experience an eight-membered H-bond pseudocycle, **1a** and **9a** form a true 'hydrazinoturn' pattern and a bifurcated hydrogen bonding network with the former having additional β-nitrogen. The stronger H-bond of the pseudocycle makes the amidic N–H bond weaker (proton more acidic), which deshields H_b and the amidic nitrogen. The chemical shifts of the amidic nitrogen of molecules **1a**, **5**, and **9a** were calculated to be 79.6, 74.6, and 82.3 ppm in the gas phase; 84.0, 81.2, and 86.6 ppm in chloroform; and 85.9, 83.9, and 88.2 ppm in water, respectively (Table S7). The nitrogen of the amidic group **1a** and **9a** is more deshielded than that of **5** as a result of bifurcated hydrogen bonding network. Compound **1a** shields more than **9a** due to back-donation by β–nitrogen. More deshielding was observed in more polar solvents favoring the unfolded state.

The formation of intramolecular hydrogen-bonds increases the magnetic deshielding of amidic nitrogen. In these cases, the intermolecular hydrogen bonds involving oxygen of carbonyl, amidic nitrogen, and proton-donor solvents contribute significantly to the total hydrogen-bonding effect; however, the former effect is more important. Hydrogen-bonds between proton-donor water and the oxygen of the amidic group show maximum deshielding effect.[20] Other factors (inductive, steric, size of pseudocycle, number of pseudocycles) also influence the chemical shift of the amidic nitrogen.

The intramolecular and intermolecular hydrogen bonds of molecules **1a** and **7a** extracted from X-ray data of Ref. 10 were compared with the hydrogen bond lengths optimized at B3LYP/6-31+G** (Figs. 8 and 9).

The information derived from the Δδ analysis appears in the solid state as **7a** crystallizes in a trimeric system, where each molecule, despite making intermolecular contacts through the amide group, is internally H-bonded with the lone-pair of the sp^3 nitrogen atom ($N^{\alpha}\cdots H_b$=2.32 Å) as postulated.[10] The optimized geometry of the trimer **7a** using the conformer of the monomer (with minimum energy) obtained from PES plot was compared with H-bonds extracted from X-ray crystallography (Fig. 8). Experimental geometry of the trimer complements the computed values with excellent accuracy. In this trimer, one molecule of **7a** acts as an H-bond donor with two other molecules and constitutes an eight-membered pseudocyclic.

In the next step, the computed bond length and torsional angles of two enantiomers of **1a** (*R*)- and (*S*)-hydrazinoturn[†] with minimum energy were compared with the X-ray structure[10] of hydrazinoturn-type arrangement (Fig. 9 and Table S9). One of the amidic protons was H-bonded with both the lone-pair of the sp^3 nitrogen atom ($N^{\alpha}\cdots$H–N=2.68 Å) and the oxygen of the carbazidic group (C=O···H–N≈2.13 Å). The experimental values of these H-bond lengths were 2.41 and 2.52 Å, respectively.[10] These values indicate much stronger H-bonds with the oxygen of C=O and a weaker interaction with N^{α} in the gas phase (these results were also verified by NBO analysis). The H-bonded hydrogen atom of the hydrazinoturn arrangement of the acetamidic methylene (NH···CH=3.60 Å) was equal to the benzylic protons (NH···CH=3.84 Å). This is in contrast to the reported experimental values of 3.08 and 4.03 Å (Fig. 9).[10]

The four torsion angles ω, φ, θ, and ψ, which characterize a (*R*)-hydrazinoturn and a (*S*)-hydrazinoturn in compound **1a**, are shown in Table S8. The slight pyramidal geometry of the N^{β} nitrogen atom

[†] (*R*)-or (*S*)-Hydrazinoturn refer to the corresponding absolute configuration of the N^{α} nitrogen atom.

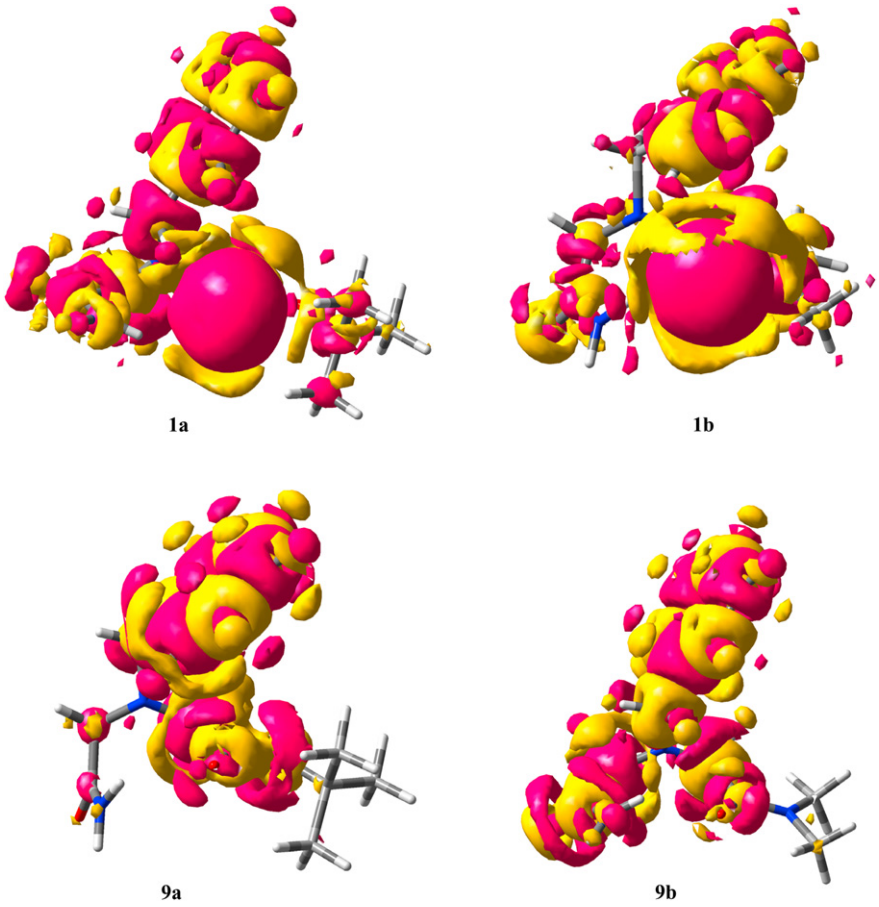

Figure 7. Depiction of the σ^* (N–H_b) orbitals of **1a**, **1b**, **9a**, and **9b**.

induces a small deviation of ω from the experimental value expected for the *Z* geometry of the carbazidic linkage. The value of the torsion angle φ permits the lone-pair of electrons of the two adjacent nitrogen atoms to adopt an orthogonal arrangement (Fig. 9a). The values taken by θ (around -122° or $+122^\circ$), which are imposed by the stronger H-bonding with the amide group, correspond to a $(-)$-synclinal or $(+)$-synclinal conformation. This places the benzyl group in a favorably less strained position (Fig. 9b). The large deviation of ψ, φ, and θ calculated values from those of experimental values reported by Salaün et al. must be the result of the degree of freedom of **1a** in the gas phase as compared with the solid phase. This demonstrates the severe danger of assuming solid-state structure has any relationship to solution-state for small flexible molecules. This flexibility allows formation of a much stronger hydrogen bond (2.13 Å) and reinforces the formation of an eight-membered pseudocycle. The experimental hydrogen bond length is 2.52 Å.

The value of 62° for ψ was calculated to be equal to four times the experiment value (14°)[10] with an opposite sign. However, these values were much smaller than those reported (140°) for *L*-β^3-

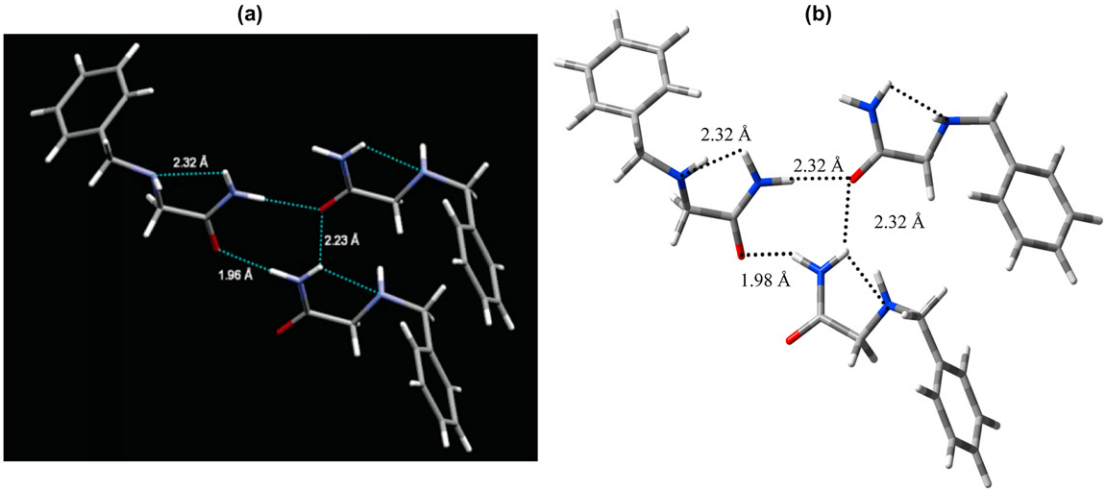

Figure 8. (a) X-ray crystal structure of trimer of **7a** (left). (b) Computed geometry of trimer of **7a** in gas phase (right).

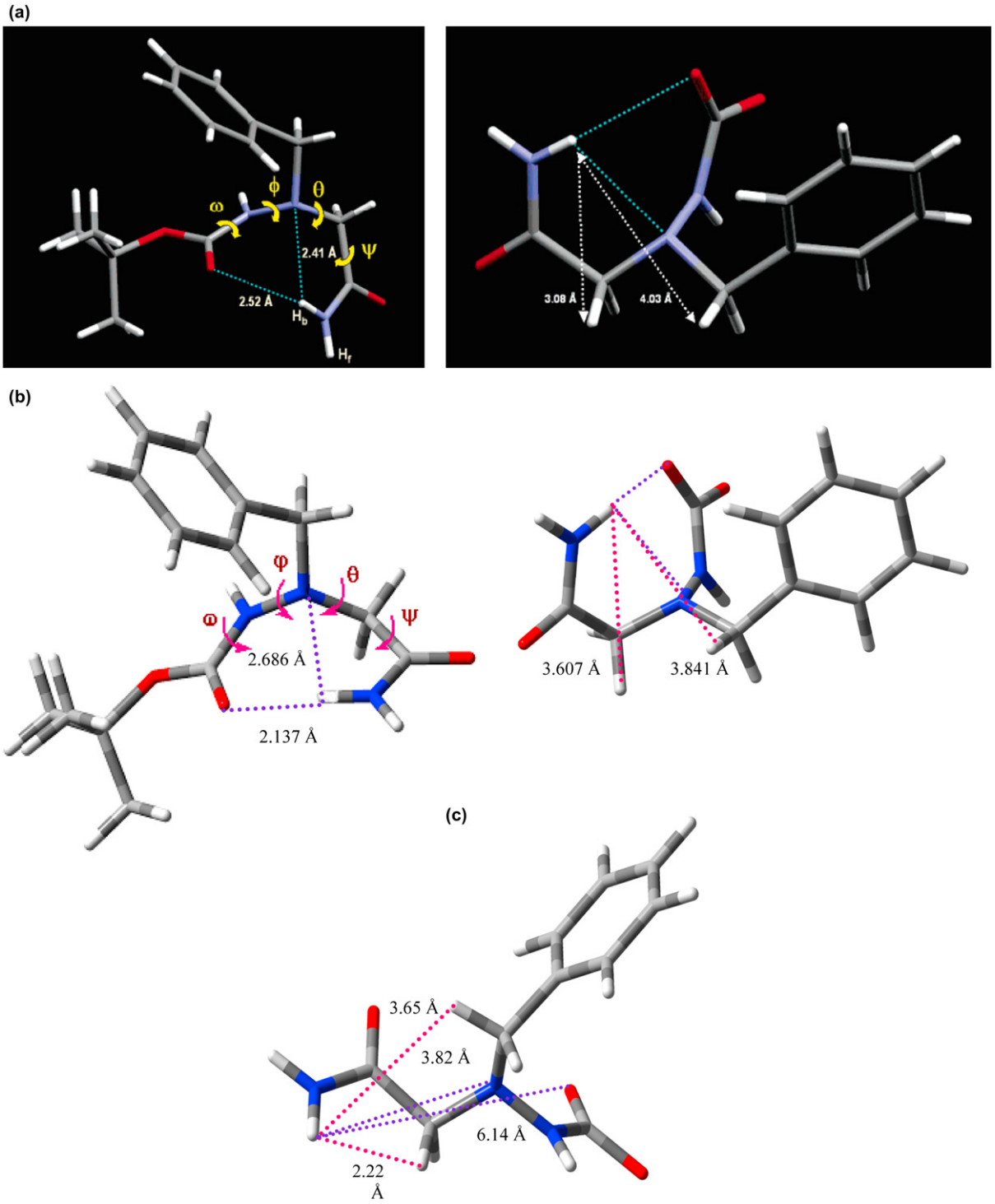

Figure 9. (a) X-ray crystal structure of **1a** H-bond length and torsional angles (left) and distances between NH_b and methylenic showing H-protons from (right).[10] The *t*-Bu group is omitted for clarity. (b) Computed minimum energy geometry of 1a H-bond length and torsional angle. (c) Conformer at dihedral angle 222° with ψ=−138° (≈−140 reported for the β^3-peptides).[6b]

peptides.[6b] The calculated high energy conformer of **1a** with a torsion angle of ψ=−138° showed no intramolecular hydrogen bonding (Fig. 9c). The computed angle ψ for the conformer at 342° are virtually the results of Ref. 10.

The projections illustrating the structural features in relationship to angles φ, θ, and ψ for a (*R*) and (*S*)-hydrazinoturn **1a** conformer with minimum energy are shown in (Fig. S3 and Scheme S1). The structural features associated with the sets of angles permit us to conclude that the hydrazinoturn conformation allows the simultaneous minimization of both steric crowding and electronic repulsion.

4. Conclusions

Our conclusions were made possible by comparing the differences in calculated and experimental chemical shift differences ($\Delta\delta$) between the geminal hydrogen atoms of the primary amide group. An excellent correlation was found between the

experimental and calculated chemical shift differences. These calculations are a valuable tool for exploring the intramolecular H-bonded systems. The total energy, H-bond length, H-bond angle, and the effect of substitution helped us to gain insight into the nature of five, six, eight, and larger pseudocycles.

The $\Delta\delta$ values (calculated from the next step, which was related to the optimized geometry) showed large deviations from those of the experimental values. However, a conformer with minimum energy from PES curve, when optimized, gave $\Delta\delta$ complementing the experimental values. Increasing polarity of the solvent (gas phase, heptane, chloroform, dimethyl sulfoxide, methanol, and water) for **3** favored the intermolecular H-bonding by shifting H_f downfield while H_b was almost unaffected (H_b predominantly is trapped by intramolecular hydrogen bonding in the folded state). The unfolded state was predominant for the compound with a weaker H-bond.

Quantum chemical study of these compounds indicated that hydrogen bonding is one of the most important factors contributing to the stabilization of these amides. A quantitative comparison between the chemical shift differences ($\Delta\delta$) values of these structures should be used with caution since the nature of the hydrogen bond acceptors, the geometry of the hydrogen bonds, the steric environment, and the size of the pseudocyle are different. The resulting H-bond gives rise to five, six, and larger ring membered hydrogen-bonded pseudocycles (bi, tri, tetra).

We believe that this work is important for future studies of hydrogen bonded systems as well as for the design of strong intermolecular interconnections. This is of crucial importance when trying to design organic systems, which are capable of interacting with other systems of interest via hydrogen bonds.

Finally, the 'hydrazinoturn' hydrogen bonding pattern appears to be a very stabilizing folding driving force, provided that the neighboring molecular functional groups do not provide other competing hydrogen bonding patterns.

Acknowledgements

The authors gratefully acknowledge the support of this work by Isfahan University of Technology (IUT) (Grant # 87/500/9143).

Supplementary data

Computed x, y, z coordinates and total energies of these molecules, structural parameters (hydrogen bond length, and hydrogen bond angle), experimental values, computed chemical shift differences of the two hydrogens of the amidic group and amidic nitrogen NMR chemical shift and their natural charges, Occupation numbers, and their related energies are given. Supplementary data associated with this article can be found in the online version doi:10.1016/j.tet.2010.02.007.

References and notes

1. Steiner, T. *Angew. Chem., Int. Ed.* **2002**, *41*, 48–76.
2. (a) Desiraju, G. R.; Steiner, T. *The Weak Hydrogen Bond in Structural Chemistry and Biology, IUCR Monographs on Crystallography*; Oxford University Press: New York NY, 1999; Vol. 9; (b) Jeffrey, G. A.; Saenger, W. *Hydrogen Bonding in Biological Structures*; Springer: Berlin, 1991; (c) Saenger, W. *Principle of Nucleic Acid Structure*; Springer: New York, NY, 1984; (d) Klebe, G. In *Structure Correlation*; Burgi, H.-B., Dunitz, J. D., Eds.; VCH: Weinheim, 1994; Vol. 2, pp 453–496.
3. Peters, D.; Peters, J. *J. Mol. Struct.* **1980**, *68*, 255–270.
4. Mitchell, J. B. O.; Price, S. L. *Chem. Phys. Lett.* **1989**, *154*, 267–272.
5. (a) Goodman, M.; Ro, S. In *Burger's Medicinal Chemistry and Drug Discovery*, 5th ed.; Wolff, M. E., Ed.; John Wiley & Sons: 1995; Vol. 1; Chapter 20, pp 803–861; (b) Ball, P. *Designing the Molecular World*; Princeton University Press: Princeton, 1994.
6. (a) Lelais, G.; Seebach, D. *Helv. Chim. Acta* **2003**, *86*, 4152–4168; (b) Seebach, D.; Beck, A. K.; Bierbaum, D. J. *Chem. Biodiversity* **2004**, *1*, 1111–1239.
7. (a) Salaün, A.; Potel, M.; Roisnel, T.; Gall, P.; Le Grel, P. *J. Org. Chem.* **2005**, *70*, 6499–6502; (b) Cheguillaume, A.; Salaün, A.; Sinbandhit, S.; Potel, M.; Gall, P.; Baudy-Floćh, M.; Le Grel, P. *J. Org. Chem.* **2001**, *66*, 4923–4929.
8. (a) Gellman, S. H. *Acc. Chem. Res.* **1998**, *31*, 173–180; (b) Hilld, J.; Mio, M. J.; Prince, R. B.; Hughes, T. S.; Moore, J. S. *Chem. Rev.* **2001**, *101*, 3893–4012; (c) Le Grel, P.; Guichard, G. In *Foldamers based on Remote Intrastrand Interactions in Foldamers*; Huc, I., Hecht, S., Eds.; Wiley-VCH: Weinheim, 2007; pp 35–74.
9. Aubry, A.; Bayeul, D.; Mangeot, J. P.; Vidal, J.; Stérin, S.; Collet, A.; Lecoq, A.; Marraud, M. *Biopolymers* **1991**, *31*, 793–801.
10. Salaün, A.; Favre, A.; Le Grel, B.; Potel, M.; Le Grel, P. *J. Org. Chem.* **2006**, *71*, 150–158.
11. Simo, C.; Salaün, A.; Arnarez, C.; Delemotte, L.; Haegy, A.; Kachma, A.; Laurent, A. D.; Thomas, J.; Jamart-Grégoire, B.; Le Grel, P.; Hocquet, A. (THEOCHEM) *J. Mol. Struct.* **2008**, *869*, 41–46.
12. (a) Dabbagh, H. A.; Teimouri, A.; Shiasi, R.; Najafi Chermahini, A. R. *J. Iran. Chem. Soc.* **2008**, *5*, 74–82; (b) Yao, L.; Vögeli, B.; Ying, J.; Bax, A. *J. Am. Chem. Soc.* **2008**, *130*, 16518–16520; (c) Timmons, C.; Wipf, P. *J. Org. Chem.* **2008**, *73*, 9168–9170.
13. (a) Dabbagh, H. A.; Noroozi-Pesyan, N.; Najafi-Chermahini, A. R.; Patrick, B. O.; James, B. R. *Can. J. Chem.* **2007**, *85*, 466–477; (b) Dabbagh, H. A.; Noroozi-Pesyan, N.; Patrick, B. O.; James, B. R. *Can. J. Chem.* **2004**, *82*, 1179–1185; (c) Kleinpeter, E.; Frank, A. *Tetrahedron* **2009**, *65*, 4418–4421; (d) JimenezFabiant, I.; Jalbout, A. F.; Moshfeghi, E.; Raissi, H. *Int. J. Quantum Chem.* **2008**, *108*, 383–390.
14. Becke, A. D. *Phys. Rev. A* **1988**, *38*, 3098–3100.
15. (a) Becke, A. D. *J. Chem. Phys.* **1993**, *98*, 5648–5652; (b) Lee, C.; Yang, W.; Paar, G. *Phys. Rev.* **1988**, *37B*, 785–789.
16. Frisch, M. J.; Trucks, G. W.; Schlegel, H. B.; Scuseria, G. E.; Robb, M. A.; Cheeseman, J. R.; Montgomery, J. A.; Vreven, J. T.; Kudin, K. N.; Burant, J. C.; Millam, J. M.; Iyengar, S. S.; Tomasi, J.; Barone, V.; Mennucci, B.; Cossi, M.; Scalmani, G.; Rega, N.; Petersson, G. A.; Nakatuji, H.; Hada, M.; Ehara, M.; Toyata, K.; Fukuda, R.; Hasegawa, J.; Ishida, M.; Nakajima, T.; Honda, Y.; Kitao, O.; Nakai, H.; Klene, M.; Li, X.; Knox, J. E.; Hratchian, H. P.; Cross, J. B.; Adamo, C.; Jaramillo, J.; Gomperts, R.; Stratmann, R. E.; Yazyev, O.; Austin, A. J.; Cammi, R.; Pomelli, C.; Ochterski, J. W.; Ayala, P. Y.; Morokuma, K.; Voth, G. A.; Salvador, P.; Dannenberg, J. J.; Zakrzewski, V. G.; Dapprich, S.; Daniels, A. D.; Strain, M. C.; Farkas, O.; Malick, D. K.; Rabuck, A. D.; Raghavachari, K.; Foresman, J. B.; Ortiz, J. V.; Cui, Q.; Baboul, A. G.; Clifford, S.; Cioslowski, J.; Stefaov, B. B.; Liu, G.; Liashenko, A.; Piskorz, P.; Komaromi, I.; Martin, R. L.; Fox, D. J.; Keith, T.; Allaham, M. A.; Peng, C. Y.; Nanaykkara, A.; Challacombe, M.; Gill, P. M. W.; Johnson, B.; Chen, W.; Wong, M. W.; Gozalez, C.; Pople, J. A. *Gaussian 03, Revision B. 05*; Gaussian,: Pittsburgh PA, 2003.
17. (a) Ditchfield, R. *Mol. Phys.* **1974**, *27*, 789–807; (b) Wolinski, K.; Hilton, J. F.; Pulay, P. *J. Am. Chem. Soc.* **1990**, *112*, 8251–8260; (c) Rauhut, G.; Puyear, S.; Wolinski, K.; Pulay, P. *J. Phys. Chem.* **1996**, *100*, 6310–6316.
18. (a) Reed, A. E.; Curtiss, L. A.; Wienhold, F. *Chem. Rev.* **1988**, *88*, 899–926; (b) Glendening, E.D.; Reed, A.E.; Carpenter, J.E.; Weinhold, F. NBO, version 3.1.
19. Dewar, M. J. S.; Jennings, W. B. *J. Am. Chem. Soc.* **1973**, *95*, 1562–1569.
20. Ksiazek, A.; Borowski, P.; Wolinski, k *J. Magn. Reson.* **2009**, *197*, 153–160.
21. H-bonding with an aromatic π-system is nevertheless possible and such interactions, commonly encountered in proteins were reviewed recently: Meyer, E. A.; Castellano, R. K.; Diederich, F. *Angew. Chem., Int. Ed.* **2003**, *42*, 1210–1250.